Thermodynamic properties and bulk viscosity near phase transition in the $Z(2)$ and $O(4)$ models

Bao-Chun Li[1,2*], Mei Huang[2,3 †]

[1] *Department of Physics, Shanxi University,Taiyuan Shanxi, China*
[2] *Institute of High Energy Physics, Chinese Academy of Sciences, Beijing, China*
[3] *Theoretical Physics Center for Science Facilities, Chinese Academy of Sciences, Beijing, China*

We investigate the thermodynamic properties including equation of state, the trace anomaly, the sound velocity and the specific heat, as well as transport properties like bulk viscosity in the $Z(2)$ and $O(4)$ models in the Hartree approximation of Cornwall-Jackiw-Tomboulis (CJT) formalism. We study these properties in different cases, e.g. first order phase transition, second order phase transition, crossover and the case without phase transition, and discuss the correlation between the bulk viscosity and the thermodynamic properties of the system. We find that the bulk viscosity over entropy density ratio exhibits an upward cusp at the second order phase transition, and a sharp peak at the 1st order phase transition. However, this peak becomes smooth or disappears in the case of crossover. This indicates that at RHIC, where there is no real phase transition and the system experiences a crossover, the bulk viscosity over entropy density might be small, and it will not affect too much on hadronization. We also suggest that the bulk viscosity over entropy density ratio is a better quantity than the shear viscosity over entropy density ratio to locate the critical endpoint.

PACS numbers: 12.38.Aw, 12.38.Mh, 51.20.+d, 51.30.+i

I. INTRODUCTION

Studying Quantum chromodynamics (QCD) phase transition and properties of hot/dense quark matter at high temperature and baryon density has been the main target of heavy ion collision experiments at the Relativistic Heavy Ion collider (RHIC), the forthcoming Large Hadron Collider (LHC) and FAIR at GSI.

At small baryon chemical potential μ, for QCD with two massless quarks, the spontaneously broken chiral symmetry is restored at finite temperature, and it is shown from lattice QCD [1] and effective QCD models [2] that this phase transition is of second order and belongs to the universality class of $O(4)$ spin model in three dimensions [3]. For real QCD with two quarks of small mass, the second order phase transition becomes a smooth crossover at finite temperature. At finite baryon chemical potential, there are still no reliable results from lattice QCD due to the severe fermion sign problem. However QCD effective models [2] suggest that the chiral phase transition at finite μ is of first order. It is expected that there exists a critical end point (CEP) in the $T-\mu$ QCD phase diagram. The CEP is defined as the end point of the first order phase transition, and belongs to the $Z(2)$ Ising universality class [4]. The precise location of the CEP is still unknown. In the future plan, RHIC is going to lower the energy and trying to locate the CEP. The signature of CEP has been suggested in Refs. [5]. Recently, the authors of Ref. [6] suggested using the shear viscosity over entropy density ratio η/s to locate the CEP .

The ratio of shear viscosity over entropy density η/s has attracted a lot of interests. It was expected that deconfined quark matter formed at high temperature should behave like a gas of weakly interacting quark-gluon plasma (wQGP). It is now believed that the system created at RHIC is a strongly coupled quark-gluon plasma (sQGP) and behaves like a nearly "perfect" fluid [7, 8]. One crucial quantity is the shear viscosity over entropy density η/s, which is required to be very small and close to the the lower bound $\eta/s = 1/4\pi$ [9] to fit the elliptic flow at RHIC from hydrodynamic simulation [10]. Lattice QCD calculation confirmed that η/s for the purely gluonic plasma is rather small and in the range of $0.1-0.2$ [11]. The perturbative QCD calculation gives a large shear viscosity in the wQGP with $\eta/s \simeq 0.8$ for $\alpha_s = 0.3$ [12]. Recent calculations using Boltzmann approach of multiparton scatterings (BAMPS) show that the small shear viscosity over entropy density can also be obtained by considering perturbative QCD inelastic scattering $gg \to ggg$, see Ref. [13].

In fluid dynamics, there is another important transport coefficient, the bulk viscosity ζ, which has often been neglected in hydrodynamic simulation of nuclear collisions. The zero bulk viscosity is for a conformal equation of state and also a reasonable approximation for the weakly interacting gas of quarks and gluons. For example, the

* libc@ihep.ac.cn
† huangm@ihep.ac.cn

perturbative QCD calculation gives $\zeta/s = 0.02\alpha_s^2$ for $0.06 < \alpha_s < 0.3$ [14]. However, recent lattice QCD results show that the bulk viscosity over entropy density ratio ζ/s rises dramatically up to the order of 1.0 near the critical temperature T_c [15, 16]. (There are still some subtle issues to determine the bulk viscosity of QCD through calculating the correlations of the energy-momentum tensor on the lattice, see more detailed discussion in Ref. [17].) The sharp peak of bulk viscosity at T_c has also been observed in the linear sigma model [18] and in the real scalar model [19]. The increasing tendency of ζ/s has been shown in a massless pion gas [20] and in the NJL model below T_c [21]. The large bulk viscosity near phase transition is related to the non-conformal equation of state [22, 23], and the correlation between the bulk viscosity and the conformal anomaly has been investigated in Ref. [24].

The sharp rise of the bulk viscosity will lead to the breakdown of the hydrodynamic approximation around the critical temperature. The effect of large bulk viscosity on hadronization and freeze-out processes of QGP created at heavy ion collisions has been discussed in Refs. [25, 26, 27, 28]. The authors of Ref. [25] pointed out the possibility that a sharp rise of bulk viscosity near phase transition induces an instability in the hydrodynamic flow of the plasma, and this mode will blow up and tear the system into droplets. Another scenario is pointed out in Ref. [15, 27] that the large bulk viscosity near phase transition might induce "soft statistical hadronization", i.e. the expansion of QCD matter close to the phase transition is accompanied by the production of many soft partons, which may be manifested through both a decrease of the average transverse momentum of the resulting particles and an increase in the total particle multiplicity.

Due to the complexity of QCD in the regime of strong coupling, results on hot quark matter from lattice calculation and hydrodynamic simulation are still lack of analytic understanding. In recent years, the anti-de Sitter/conformal field theory (AdS/CFT) correspondence has generated enormous interest in using thermal $\mathcal{N} = 4$ super-Yang-Mills theory (SYM) to understand sQGP. The shear viscosity to entropy density ratio η/s is as small as $1/4\pi$ in the strongly coupled SYM plasma [9]. However, a conspicuous shortcoming of this approach is the conformality of SYM: the square of the speed of sound c_s^2 always equals to $1/3$ and the bulk viscosity is always zero at all temperatures in this theory. Though ζ/s at T_c is non-zero for a class of black hole solutions resembling the equation of state of QCD, the magnitude is less than 0.1 [29], which is too small comparing with lattice QCD results.

An alternative nonperturbative approach to study QCD phase transition is by using effective models. There is still no satisfied dynamic model which can describe deconfinement phase transition successfully. We thus focus on effective models which can describe chiral symmetry restoration. QCD with two-flavor massless quarks has a global symmetry $SU(2)_R \times SU(2)_L$, which is isomorphic to $O(4)$. The chiral symmetry restoration in the case of 2-flavor QCD is of second order phase transition, and the universal critical behavior falls in the same universality class as the $O(4)$ model [3]. It has been argued that the chiral phase transition at finite chemical potential near critical point belongs to the $Z(2)$ universality class [4]. This motivates us to study the thermodynamic and transport properties of $Z(2)$ and $O(4)$ models near phase transition in this paper.

The critical phenomena in the $Z(2)$ and $O(4)$ models have been well-known, and the singular behavior of the static and dynamic properties has been very well studied. However, due to the finite size and time effects for the system created in heavy ion collisions, the critical singularity will not show up in the observables. Therefore, in this paper, we will not focus on the singularities at the critical point. We will study the thermodynamic and transport properties in the Hartree approximation of the Cornwall-Jackiw-Tomboulis (CJT) formalism [30]. At finite temperature, the naive perturbative expansion in powers of the coupling constant breaks down, and CJT formalism provides a convenient resummation method. In the Hartree approximation, we cannot perform the precise critical behavior at phase transition, but we can get the qualitative behavior near phase transition.

It has been found in Ref. [31] that in the simplest real scalar model with $Z(2)$ symmetry breaking in the vacuum, η/s behaves the same way as that in systems of water, helium and nitrogen in first-, second-order phase transitions and crossover [32]. In Ref. [19], we have investigated the equation of state and bulk viscosity in the real scalar model in the case of 2nd order phase transition, and we have found that the thermodynamic properties and transport properties in this simple model at strong coupling are similar to those of the complex QCD system. In this paper, we will systematically investigate the thermodynamic properties and bulk viscosity of the $Z(2)$ model and the $O(4)$ model in the cases of first-, second-order phase transitions and crossover in the framework of CJT formalism.

This paper is organized as follows. In Sec. II, we introduce the CJT formalism in the $Z(2)$ and $O(4)$ model. In Sec. III, we introduce the thermodynamic quantities and the bulk viscosity. In Sec. IV, we present our numerical results. At the end, we give discussions and summary in Sec. V.

II. $Z(2)$ AND $O(4)$ MODELS IN THE FRAMEWORK OF CJT FORMALISM

A. CJT formalism

At finite temperature T, the temperature introduces a new energy scale which can conspire with the typical momentum scale p of a process so that gT/p is no longer of order g, but can be of order 1 [33]. Consequently, all terms of order gT/p have to be taken into account which requires the resummation of certain classes of diagrams. The CJT formalism, which is equivalent to the Φ-functional approach of Luttinger and Ward [34] and Baym [35], provides such a convenient resummation method. In this paper, we follow the notations used in Ref. [36].

The CJT formalism can be viewed as a prescription for computing the effective action of a given theory, it generalizes the concept of the effective action $\Gamma[\bar{\phi}]$ for the expectation value $\bar{\phi}$ of the one-point function in the presence of external sources to that for the effective action $\Gamma[\bar{\phi},\bar{G}]$ for $\bar{\phi}$ and the expectation value $\bar{G}$ of the two-point function in the presence of external sources, with

$$\Gamma[\bar{\phi},\bar{G}] = \Gamma_0[\bar{\phi}] + \frac{1}{2}\,\mathrm{Tr}\ln\bar{G}^{-1} + \frac{1}{2}\mathrm{Tr}(G_0^{-1}\bar{G}-1) + \Gamma_2[\bar{\phi},\bar{G}]. \tag{1}$$

Here, $\Gamma_0[\bar{\phi}]$ is the tree-level action, G_0^{-1} the inverse tree-level two-point function, and $\Gamma_2[\bar{\phi},\bar{G}]$ the sum of all two-particle irreducible (2PI) vacuum diagrams with internal lines given by $\bar{G}$.

The stationary points of this functional,

$$\left.\frac{\delta\Gamma[\bar{\phi},\bar{G}]}{\delta\bar{\phi}}\right|_{\bar{\phi}=\varphi,\bar{G}=G} = 0\ , \qquad \left.\frac{\delta\Gamma[\bar{\phi},\bar{G}]}{\delta\bar{G}}\right|_{\bar{\phi}=\varphi,\bar{G}=G} = 0\ , \tag{2}$$

provide self-consistent equations for the expectation values of the one- and two-point functions $\bar{\phi}$ and $\bar{G}$ in the absence of external sources, denoted as φ and G, respectively. The stationarity conditions Eq. (2) for the effective action are Dyson-Schwinger equations for the one- and two-point Green's functions of the theory. The Dyson-Schwinger equation for the two-point Green's function can be derived and has the form of

$$G^{-1} = G_0^{-1} + \Pi\ , \tag{3}$$

where

$$\Pi \equiv -2\ \left.\frac{\delta\Gamma_2[\bar{\phi},\bar{G}]}{\delta\bar{G}}\right|_{\bar{\phi}=\varphi,\bar{G}=G} \tag{4}$$

is the self-energy.

In general, the CJT formalism resums one-particle irreducible diagrams to all orders. As long as Γ_2 contains all 2PI diagrams, the CJT effective action is exact. However, it is practically impossible to compute all 2PI diagrams, and one has to truncate Γ_2 at some order in the number of loops. The advantage of the CJT formalism is that any truncation of Γ_2 yields a many-body approximation scheme which preserves the symmetries of the tree-level action. The solution of Eqs. (2) is thermodynamically consistent and conserves the Noether currents.

The CJT formalism is quite useful for studying theories with spontaneously broken symmetries. In the following, we use the CJT formalism studying the $Z(2)$ and $O(4)$ models with spontaneous symmetry breaking in the vacuum and symmetry restoration at finite temperature.

B. $Z(2)$ model in the CJT formalism

The critical end point has been studied by using the Ginzburg-Landau effective potential of the order parameter field (scalar field) up to the sixth order, e.g. see Ref. [4]. Here we introduce the real scalar theory including the sextet interaction which described by the Lagrangian

$$\mathcal{L} = \frac{1}{2}(\partial_\mu\phi)^2 - \frac{1}{2}a\phi^2 - \frac{1}{4}b\phi^4 - \frac{1}{6}c\phi^6 + H\phi. \tag{5}$$

When $H=0$, this theory is invariant under $\phi\to-\phi$ and has a Z_2 symmetry.

Unlike in the Ginzburg-Landau effective potential [4] where a,b,c are functions of temperature, here a,b,c are model parameters, which determine the vacuum properties. The system at finite temperature will be evaluated in the CJT formalism. We will discuss the following four cases: 1) $c=0, b>0, a>0, H=0$, the system is always in the symmetric

phase. 2) $c=0, b>0, a<0, H=0$, the vacuum at $T=0$ breaks the Z_2 symmetry spontaneously, and the symmetry is restored at higher T with a second-order phase transition. 3) $c=0, b>0, a<0, H\neq 0$, the $Z(2)$ symmetry is explicitly broken, and the system will experience a crossover at high temperature. 4) $c>0, b<0, a>0, H=0$, the broken symmetry is restored at high T with a first-order phase transition.

Assuming translation invariance, we consider effective potential Ω instead of effective action Γ, these two quantities are related via:

$$\Gamma = -\frac{V}{T}\Omega, \tag{6}$$

where V is the 3-volume of the system. The effective potential in the CJT formalism reads [36]

$$\Omega[\bar{\phi},\bar{G}] = \Omega_0(\bar{\phi}) + \frac{1}{2}\int_K \left[\ln \bar{G}^{-1}(K) + \bar{G}_0^{-1}(K)\,\bar{G}(K) - 1\right] + \Omega_2[\bar{\phi},\bar{G}], \tag{7}$$

where

$$\Omega_0(\bar{\phi}) = \frac{a}{2}\,\bar{\phi}^2 + \frac{b}{4}\,\bar{\phi}^4 + \frac{c}{6}\,\bar{\phi}^6 - H\bar{\phi} \tag{8}$$

is the tree-level potential, and $\bar{G}(\bar{G}_0)$ is the full(tree-level) propagator:

$$\bar{G}^{-1}(K,\bar{\phi}) = -K^2 + m^2(\bar{\phi})\,, \bar{G}_0^{-1}(K,\bar{\phi}) = -K^2 + m_0^2(\bar{\phi})\,, \tag{9}$$

with the tree-level mass $m_0^2 = a + 3b\,\bar{\phi}^2 + 5c\,\bar{\phi}^4$. In Hartree approximation, the 2PI potential Ω_2 only includes

$$\Omega_2[\bar{\phi},\bar{G}] = \left(\frac{3}{4}b + \frac{15}{2}c\bar{\phi}^2\right)\left(\int_K \bar{G}(K)\right)^2 + \frac{15}{6}c\left(\int_K \bar{G}(K)\right)^3, \tag{10}$$

The self-consistent one- and two-point Green's functions satisfy

$$\left.\frac{\delta\Omega}{\delta\bar{\phi}}\right|_{\bar{\phi}=\phi,\bar{G}=G} \equiv 0\,, \quad \left.\frac{\delta\Omega}{\delta\bar{G}}\right|_{\bar{\phi}=\phi,\bar{G}=G} \equiv 0 \quad . \tag{11}$$

This allows us to solve ϕ and m through the coupled Dyson-Schwinger equations:

$$\begin{aligned} a\phi + b\phi^3 + c\phi^5 + (3b\phi + 10c\phi^3)\int_K G(K) + 15c\phi\left(\int_K G(K)\right)^2 &= H\,, \\ m^2 - m_0^2 = 3(b + 10c\phi^2)\int_K G(K) + 15c\left(\int_K G(K)\right)^2 &. \end{aligned} \tag{12}$$

C. $O(4)$ model in the CJT formalism

The Lagrangian of the $O(N)$ model reads

$$\mathcal{L}(\phi) = \frac{1}{2}\,\partial_\mu\boldsymbol{\phi}\cdot\partial^\mu\boldsymbol{\phi} - \frac{a}{2}\boldsymbol{\phi}\cdot\boldsymbol{\phi} - \frac{b}{4N}(\boldsymbol{\phi}\cdot\boldsymbol{\phi})^2 + H\phi_1 \quad , \tag{13}$$

where $\boldsymbol{\phi} \equiv (\phi_1, ..., \phi_N)$ is an $O(N)$ vector. We identify the first component ϕ_1 with the σ field and the remaining $N-1$ components as the π fields. The last term $H\phi_1$ breaks the symmetry explicitly and has been introduced in order to generate masses for the pions. For $H=0$, $a>0$ and $b>0$, the Lagrangian is invariant under $O(N)$ rotations of the fields. For $H=0$, $a<0$ and $b>0$, this symmetry is spontaneously broken down to $O(N-1)$, leading to $N-1$ Goldstone bosons (the pions), and the field $\boldsymbol{\phi}$ obtains a non-vanishing vacuum expectation value $\bar{\phi}$. The $O(N)$ symmetry will be restored at finite temperature with a second-order phase transition. By shifting the field as $\boldsymbol{\phi} \to \boldsymbol{\phi} + \bar{\phi}$, the "classical potential" takes the form

$$\Omega_0(\bar{\phi}) \;=\; \frac{a}{2}\bar{\phi}^{\,2} + \frac{b}{4N}\bar{\phi}^{\,4} - H\bar{\phi} \quad . \tag{14}$$

The inverse tree-level propagator which corresponds to the above Lagrangian density is

$$\bar{G}_{0\sigma}^{-1}(k;\bar{\phi}) \;=\; -k^{\,2} + a + \frac{3\,b}{N}\,\bar{\phi}^{\,2} \quad , \tag{15}$$

$$\bar{G}_{0\pi}^{-1}(k;\bar{\phi}) \;=\; -k^{\,2} + a + \frac{b}{N}\,\bar{\phi}^{\,2} \quad , \tag{16}$$

where $G_{0\sigma}^{-1}, G_{0\pi}^{-1}$ are sigma and pion propagator respectively.

The CJT effective potential of the $O(N)$ model can be written as the following function of full propagators:

$$\begin{aligned}\Omega(\bar{\phi},\bar{G}_\sigma,\bar{G}_\pi) \;=\; & \Omega_0(\bar{\phi}) + \frac{1}{2}\int_k \left[\ln \bar{G}_\sigma^{-1}(k) + \bar{G}_{0\sigma}^{-1}(k;\bar{\phi})\,\bar{G}_\sigma(k) - 1\right] \\ & + \frac{N-1}{2}\int_k \left[\ln \bar{G}_\pi^{-1}(k) \,+ \bar{G}_{0\pi}^{-1}(k;\bar{\phi})\,\bar{G}_\pi(k) - 1\right] \,+ \Omega_2(\bar{\phi},\bar{G}_\sigma,\bar{G}_\pi) \quad .\end{aligned} \tag{17}$$

In the Hartree approximation, the 2PI effective potential Ω_2 takes the form of

$$\Omega_2 = (N+1)(N-1)\,\frac{b}{4N}\left[\int_Q \bar{G}_\pi(Q)\right]^2 + 3\,\frac{b}{4N}\left[\int_Q \bar{G}_\sigma(Q)\right]^2 + 2\,(N-1)\frac{b}{4N}\int_Q \bar{G}_\sigma(Q)\int_L \bar{G}_\pi(L)\;. \tag{18}$$

The stationarity condition is written as

$$\left.\frac{\delta\Omega[\bar{\phi},\bar{G}_\sigma,\bar{G}_\pi]}{\delta\bar{\phi}}\right|_{\bar{\phi}=\phi,\,\bar{G}_\sigma=G_\sigma,\,\bar{G}_\pi=G_\pi} = 0 \quad , \tag{19}$$

$$\left.\frac{\delta\Omega[\bar{\phi},\bar{G}_\sigma,\bar{G}_\pi]}{\delta\bar{G}_\sigma(k)}\right|_{\bar{\phi}=\phi,\,\bar{G}_\sigma=G_\sigma,\,\bar{G}_\pi=G_\pi} = 0 \quad , \tag{20}$$

$$\left.\frac{\delta\Omega[\bar{\phi},\bar{G}_\sigma,\bar{G}_\pi]}{\delta\bar{G}_\pi(k)}\right|_{\bar{\phi}=\phi,\,\bar{G}_\sigma=G_\sigma,\,\bar{G}_\pi=G_\pi} = 0 \quad , \tag{21}$$

which determines the expectation values of the one- and two-point functions in the absence of external sources ϕ and G_σ, G_π. Similarly, the Schwinger–Dyson equations for sigma and pion propagators for the effective potential Ω are given by

$$G_\sigma^{-1}(k) \;=\; G_{0\sigma}^{-1}(k;\phi) + \Sigma_\sigma(k) \;= -k^2 + M_\sigma^2 \;, \tag{22}$$

$$G_\pi^{-1}(k) \;=\; G_{0\pi}^{-1}(k;\phi) + \Sigma_\pi(k) \;= -k^2 + M_\pi^2 \;. \tag{23}$$

By solving Eq.(20) and (21), the corresponding self-energy can be obtained as

$$\Sigma_\sigma(k) \equiv \quad 2\,\left.\frac{\delta\Omega_2[\bar{\phi},\bar{G}_\sigma,\bar{G}_\pi]}{\delta\bar{G}_\sigma(k)}\right|_{\bar{\phi}=\phi,\,\bar{G}_\sigma=G_\sigma,\,\bar{G}_\pi=G_\pi} \quad , \tag{24}$$

$$\Sigma_\pi(k) \equiv \quad \frac{2}{N-1}\,\left.\frac{\delta\Omega_2[\bar{\phi},\bar{G}_\sigma,\bar{G}_\pi]}{\delta\bar{G}_\pi(k)}\right|_{\bar{\phi}=\phi,\,\bar{G}_\sigma=G_\sigma,\,\bar{G}_\pi=G_\pi} \quad . \tag{25}$$

In our following numerical calculations, we will take the case of $N = 4$.

III. THE EQUATION OF STATE, SOUND VELOCITY, SPECIFIC HEAT, INTERACTION MEASURE AND BULK VISCOSITY

Once we have the effective potential Ω, we can derive all thermodynamic properties of the system. The entropy density is determined by taking the derivative of effective potential with respect to the temperature, i.e,

$$s = -\partial\Omega(\phi)/\partial T. \tag{26}$$

In the symmetry breaking case, the vacuum effective potential or the vacuum energy density is negative, i.e,

$$\Omega_v = \Omega(\phi)|_{T=0} < 0. \tag{27}$$

As the standard treatment in lattice calculation, we introduce the normalized pressure density p_T and energy density ϵ_T as

$$p_T = -\Omega_T,\ \epsilon_T = -p_T + Ts, \tag{28}$$

with

$$\Omega_T = \Omega(\phi) - \Omega_v. \tag{29}$$

The equation of state $p_T(\epsilon_T)$ is an important input into hydrodynamics. The square of the speed of sound C_s^2 is related to p_T/ϵ_T and has the form of

$$C_s^2 = \frac{\mathrm{d}p}{\mathrm{d}\epsilon} = \frac{s}{T\mathrm{d}s/\mathrm{d}T} = \frac{s}{C_v}, \tag{30}$$

where

$$C_v = \partial\epsilon/\partial T, \tag{31}$$

is the specific heat. At the critical temperature, the entropy density as well as the energy density change most quickly with temperature, thus one expect that C_s^2 should have a minimum at T_c. The trace anomaly of the energy-momentum tensor $\mathcal{T}^{\mu\nu}$

$$\Delta = \frac{\mathcal{T}^{\mu\mu}}{T^4} \equiv \frac{\epsilon_T - 3p_T}{T^4} = T\frac{\partial}{\partial T}(p_T/T^4) \tag{32}$$

is a dimensionless quantity, which is also called the "interaction measure".

The bulk viscosity is related to the correlation function of the trace of the energy-momentum tensor θ^μ_μ:

$$\zeta = \frac{1}{9}\lim_{\omega\to 0}\frac{1}{\omega}\int_0^\infty dt\int d^3r\, e^{i\omega t}\left\langle[\theta^\mu_\mu(x), \theta^\mu_\mu(0)]\right\rangle. \tag{33}$$

According to the result derived from low energy theorem, in the low frequency region, the bulk viscosity takes the form of [15]

$$\begin{aligned}\zeta &= \frac{1}{9\,\omega_0}\left\{T^5\frac{\partial}{\partial T}\frac{(\epsilon_T - 3p_T)}{T^4} + 16|\epsilon_v|\right\},\\ &= \frac{1}{9\,\omega_0}\left\{-16\epsilon_T + 9TS + TC_v + 16|\epsilon_v|\right\}.\end{aligned} \tag{34}$$

with the negative vacuum energy density $\epsilon_v = \Omega_v = \Omega(\phi)|_{T=0}$, and the parameter $\omega_0 = \omega_0(T)$ is a scale at which the perturbation theory becomes valid. From the above formula, we can see that the bulk viscosity is proportional to the specific heat C_v near phase transition, thus ζ/s behaves as $1/C_s^2$ near T_c in this appproximation.

IV. THERMODYNAMIC PROPERTIES OF $Z(2)$ AND $O(4)$ MODELS

In this section, we show our numerical results for thermodynamic properties of the $Z(2)$ and $O(4)$ models.

A. $Z(2)$ model without symmetry breaking in the vacuum

We firstly consider the real scalar model without symmetry breaking in the vacuum, i.e. $a > 0$. In Fig. 1 $(a)-(e)$, we show the ratio of the pressure density over energy density p_T/ϵ_T, the trace anomaly $(\epsilon_T - 3p_T)/T^4$, the square of sound velocity C_s^2, the specific heat C_v and the bulk viscosity over entropy density ratio ζ/s as functions of the temperature T for different coupling strength b. The parameters taken for calculations are: 1) $a = 1000\,\mathrm{MeV}^2$, $b = 0.1$, 2) $a = 10000\,\mathrm{MeV}^2$, $b = 10$, 3) $a = 10000\,\mathrm{MeV}^2$, $b = 30$, and 4) $a = 10000\,\mathrm{MeV}^2$, $b = 60$.

In the weak coupling case when $b = 0.1$, it is found that the pressure density over energy density p_T/ϵ_T, the sound velocity square C_s^2 and the specific heat C_v show similar behavior as in the ideal gas. Both p_T/ϵ_T and C_s^2 increase with the temperature T, and reach the conformal value 1/3 at high temperature. The specific heat C_v monotonically increases with temperature. There is no much information about the trace anomaly $(\epsilon_T - 3p_T)/T^4$ for an ideal gas

in the literature. It is found that the trace anomaly $(\epsilon_T - 3p_T)/T^4$ shows a peak at low temperature, then decreases monotonically and reaches the conformal value 0 at high temperature.

The peak of the trace anomaly $(\epsilon_T - 3p_T)/T^4$ at low temperature, which is not related to the phase transition was also observed in Ref. [19] in the real scalar model with 2nd-order phase transition and in Ref. [24] in the Chiral Perturbation Theory for the pion gas. In Ref. [24], the low-T peak of the trace anomaly was interpreted as the explicit conformal breaking, whose contribution comes from massive pions. However, for the real scalar system, there are no massive pions, it is not clear for us what is the reason inducing the conformal symmetry breaking at low temperature.

In the case of strong coupling, we observe that the pressure density over energy density p_T/ϵ_T, the sound velocity square C_s^2 increase with temperature and saturate at high temperature. The pressure density over energy density p_T/ϵ_T saturates at a value smaller than 1/3, the stronger the coupling strength is, the smaller value p_T/ϵ_T saturates. The sound velocity square C_s^2 still saturates at 1/3. The specific heat C_v increases with temperature. However, it is found that the low-T peak of the trace anomaly slowly disappears with the increase of the coupling strength, and at high T, the trace anomaly goes to a larger value for stronger coupling strength b, which indicates that the conformal symmetry is broken at high T due to the bare strong coupling. Therefore, the trace anomaly at high temperature can indicate the strength of the coupling, in this sense, the trace anomaly is also called the "interaction measure".

In both weak coupling and strong coupling, the bulk viscosity over entropy density ζ/s decreases monotonically with the increase of the temperature. At high T, ζ/s reaches its conformal value 0 in the case of weak coupling, and reaches a finite value in the case of strong coupling. However, we don't observe the correlation between the trace anomaly and the bulk viscosity as shown in Ref. [24], where it shows that the peak at low temperature in the trace anomaly also appears in the bulk viscosity.

B. $Z(2)$ model with a second-order phase transition

In Fig. 2 $(a)-(e)$, we show the ratio of pressure density over energy density p_T/ϵ_T, the trace anomaly $(\epsilon_T-3p_T)/T^4$, the sound velocity square C_s^2, the specific heat C_v and the bulk viscosity over entropy density ζ/s as functions of the temperature T for different coupling strength b for the real scalar model with a second order phase transition. The parameters used for calculations and the corresponding critical temperatures are: 1) $a = -100\,\mathrm{MeV}^2$, $b = 0.1$, $T_c = 88\,\mathrm{MeV}$, 2) $a = -10000\,\mathrm{MeV}^2$, $b = 10$, $T_c = 82\,\mathrm{MeV}$, 3) $a = -50000\,\mathrm{MeV}^2$, $b = 30$, $T_c = 124\,\mathrm{MeV}$, 4) $a = -100000\,\mathrm{MeV}^2$, $b = 60$, $T_c = 144\,\mathrm{MeV}$. The main results in this case have been shown in Ref. [19].

In the weak coupling case when $b = 0.1$, it is found that the pressure density over energy density p_T/ϵ_T, the sound velocity square C_s^2 and the specific heat C_v show similar behavior as in the ideal gas except near the phase transition region. Both p_T/ϵ_T and C_s^2 show a downward cusp at T_c, and reach the conformal value 1/3 at high temperature. The specific heat C_v exhibits a small upward cusp at T_c. In the weak coupling case, we observe double peak in the trace anomaly, one smooth peak shows up at low temperature, another upward cusp appears at T_c.

In the case of strong coupling, at high temperature region $T > T_c$, the behavior of the the pressure density over energy density p_T/ϵ_T, the sound velocity square C_s^2, the specific heat C_v, and the trace anomaly show similar behavior as those in the symmetric case. p_T/ϵ_T and C_s^2 increase with temperature and saturate at high temperature. The pressure density over energy density p_T/ϵ_T saturates at a value smaller than 1/3, the stronger the coupling strength is, the smaller saturation value p_T/ϵ_T will be. The sound velocity square C_s^2 still saturates at 1/3. The specific heat C_v increases with temperature. The trace anomaly decreases with temperature and goes to a larger value for stronger coupling strength b.

Near phase transition region $T \simeq T_c$, both the pressure density over energy density p_T/ϵ_T and the sound velocity square C_s^2 show a downward cusp at T_c, the specific heat C_v and the trace anomaly show an upward cusp at T_c. When the coupling strength increases, the depth of the downward cusp for the pressure density over energy density p_T/ϵ_T and the sound velocity square C_s^2 become deeper and deeper, while the height of the upward cusp for the specific heat C_v and the trace anomaly becomes higher and higher.

At low temperature region $T < T_c$, both the pressure density over energy density p_T/ϵ_T and the sound velocity square C_s^2 show a bump, i.e. p_T/ϵ_T and C_s^2 firstly increase with T then decrease with T. However, it is found that the low-T peak of the trace anomaly slowly disappears with the increase of the coupling strength.

The bulk viscosity over entropy density ζ/s decreases with T at low temperature region, then rises up at the critical temperature T_c, and decreases further in the temperature $T > T_c$.

C. $Z(2)$ model with explicit symmetry breaking

In Fig. 3 $(a)-(e)$, we show the ratio of pressure density over energy density p_T/ϵ_T, the sound velocity square C_s^2, the trace anomaly $(\epsilon_T - 3p_T)/T^4$, the specific heat C_v and the bulk viscosity over entropy density ζ/s as functions of

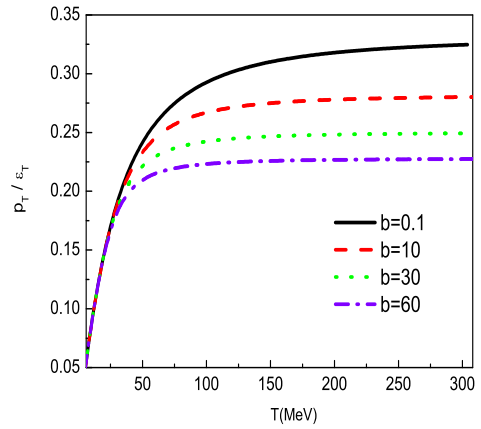

(a)

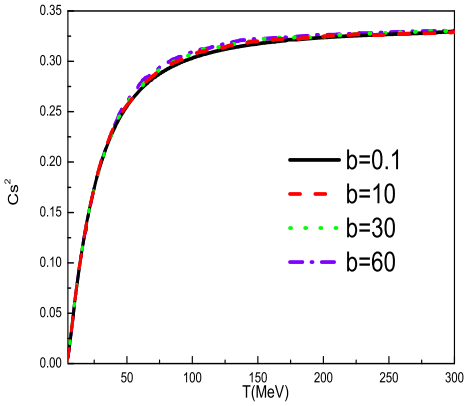

(b)

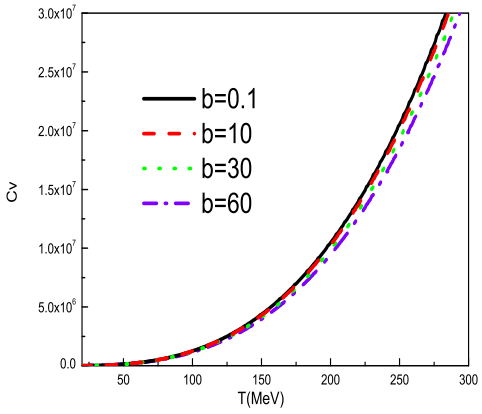

(c)

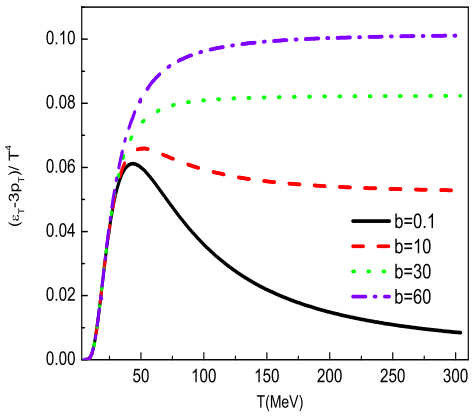

(d)

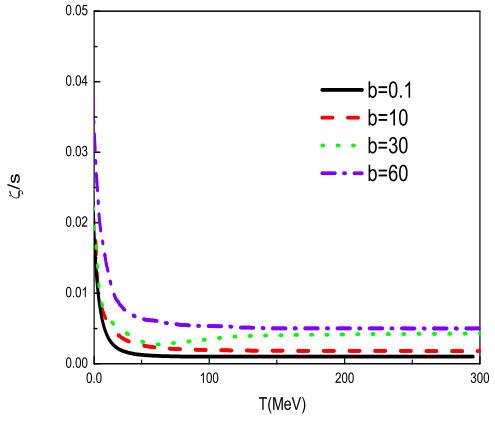

(e)

FIG. 1: The ratio of pressure density over energy density p_T/ϵ_T, the trace anomaly $(\epsilon_T - 3p_T)/T^4$, the sound velocity square C_s^2, the specific heat C_v and the bulk viscosity over entropy density ratio ζ/s as functions of the temperature T for the real scalar model in the symmetric phase.

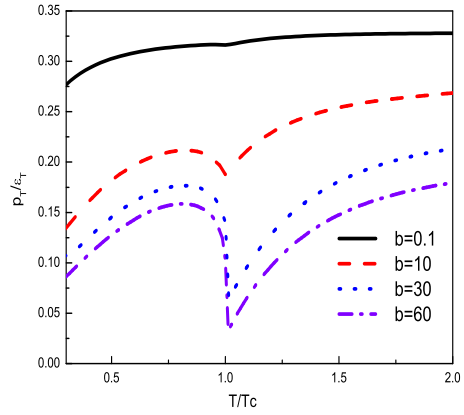

(a)

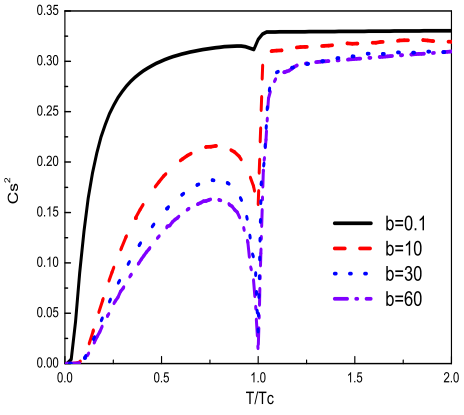

(b)

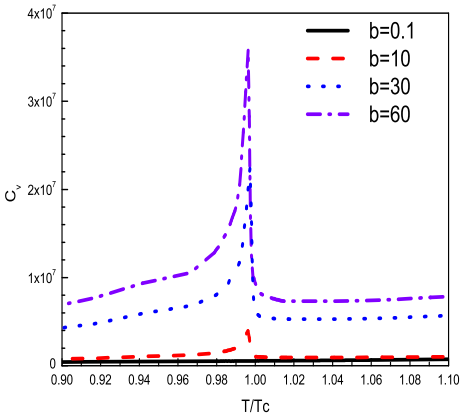

(c)

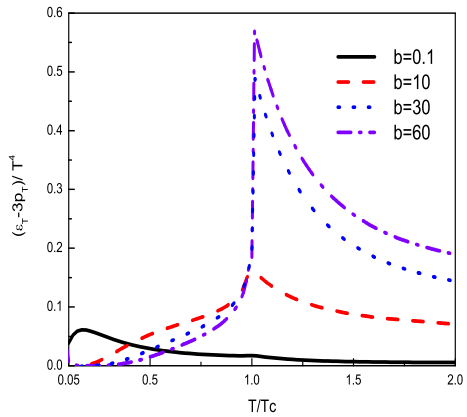

(d)

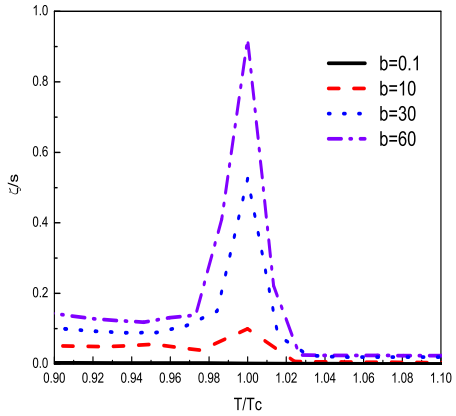

(e)

FIG. 2: The ratio of pressure density over energy density p_T/ϵ_T, the trace anomaly $(\epsilon_T - 3p_T)/T^4$, the sound velocity square C_s^2, the specific heat C_v and the bulk viscosity over entropy density ratio ζ/s as functions of the temperature T with a second-order phase transition in the real scalar model.

the temperature T for second order phase transition and crossover for the real scalar model. The parameters used for calculations are: 1) $a = -10000\,\mathrm{MeV}^2$, $b = 10$, $H = 0$, and 2) $a = -10000\,\mathrm{MeV}^2$, $b = 10$, $H = (40\mathrm{MeV})^3$. The only difference of the two set of parameters is the value of H. When $H = 0$, the system experiences a second order phase transition, and when $H \neq 0$, the system experiences a crossover.

At both low temperature region $T < T_c$ and high temperature region $T > T_c$, the behavior of all the thermodynamic quantities and bulk viscosity don't show much difference for these two set of parameters. However, near critical temperature region $T \simeq T_c$, it is observed all the cusp behaviors are washed out, e.g. the downward cusp in the pressure density over energy density p_T/ϵ_T and the sound velocity square C_s^2 develops into a shallow valley, and the upward cusp in the trace anomaly develops into a smooth peak. Especially, the upward cusp for the specific heat C_v and the bulk viscosity over entropy density ζ/s vanishes and there is no obvious change near critical temperature.

D. $Z(2)$ model with a first-order phase transition

In Fig. 4 $(a)-(e)$, we show the ratio of pressure density over energy density p_T/ϵ_T, the sound velocity square C_s^2, the trace anomaly $(\epsilon_T - 3p_T)/T^4$, the specific heat C_v and the bulk viscosity over entropy density ζ/s as functions of the temperature T for the real scalar model with a first order phase transition. The parameters used for calculations and corresponding critical temperatures are: 1) $a = 100\,\mathrm{MeV}^2$, $b = -0.125$, $c = 0.000025\,\mathrm{MeV}^{-2}$, $T_c = 59$ MeV, 2) $a = 10000\,\mathrm{MeV}^2$, $b = -1.2$, $c = 0.000025\,\mathrm{MeV}^{-2}$, $T_c = 155\,\mathrm{MeV}$, 3) $a = 40000\,\mathrm{MeV}^2$, $b = -4$, $c = 0.000069\,\mathrm{MeV}^{-2}$, $T_c = 204\,\mathrm{MeV}$.

At high temperature region $T > T_c$, the behavior of the pressure density over energy density p_T/ϵ_T, the sound velocity square C_s^2, the specific heat C_v, and the trace anomaly show similar behavior as those in the case of symmetric phase. p_T/ϵ_T and C_s^2 increase with temperature and saturate at the conformal value 1/3 at high temperature. The specific heat C_v increases with temperature and the trace anomaly decreases with temperature and goes to the conformal value 0.

At low temperature region $T < T_c$, the behavior of the pressure density over energy density p_T/ϵ_T, the sound velocity square C_s^2, the specific heat C_v, and the trace anomaly also show similar behavior as those in the case of symmetric phase. Both the pressure density over energy density p_T/ϵ_T and the sound velocity square C_s^2 monotonically increase with the temperature. The low-T peak of the trace anomaly still shows up in the weak coupling case and slowly disappears with the increase of the coupling strength.

Near phase transition region $T \simeq T_c$, the behavior of the pressure density over energy density p_T/ϵ_T, the sound velocity square C_s^2, the specific heat C_v, and the trace anomaly also show similar behavior as those in the case of second order phase transition. The only difference is that the width of the cusp becomes very narrow. The downward cusp in the pressure density over energy density p_T/ϵ_T and the sound velocity square C_s^2 becomes a dip at T_c, and the upward cusp of the specific heat C_v and the trace anomaly develops into a delta function at T_c. When the coupling strength increases, the value of the pressure density over energy density p_T/ϵ_T and the sound velocity square C_s^2 at T_c become smaller and smaller, while the value of the specific heat C_v and the trace anomaly becomes bigger and bigger.

The bulk viscosity over entropy density ζ/s decreases with T at low temperature region, then sharply rises up at the critical temperature T_c, and decreases further in the temperature $T > T_c$. The value of ζ/s becomes larger and larger at the critical temperature with the increase of coupling strength.

E. $O(4)$ model with spontaneous symmetry breaking in the vacuum

In Fig. 5 $a-e$, we show the ratio of pressure density over energy density p_T/ϵ_T, the sound velocity square C_s^2, the interaction measure $(\epsilon_T - 3p_T)/T^4$, the specific heat C_v and the bulk viscosity over entropy density ζ/s as functions of the temperature T for the $O(4)$ model with a second order phase transition in the chiral limit $H = 0$. The parameters used for calculation are taken from [37]: 1) $a = -(282.84\mathrm{MeV})^2$, $b = 39.53$, 2) $a = -(424.264\mathrm{MeV})^2$, $b = 88.88$, and 3) $a = -(565.685\mathrm{MeV})^2$, $b = 158.02$ which produce the vacuum pion mass $m_\pi = 0$, vacuum pion decay constant $f_\pi = 90\,\mathrm{MeV}$, and vacuum sigma meson mass as $m_\sigma = 400\mathrm{MeV}$ $m_\sigma = 600\mathrm{MeV}$ and $m_\sigma = 800\mathrm{MeV}$, respectively. The stronger coupling strength of b corresponds to the larger sigma mass in the vacuum. The critical temperature for the chiral symmetry restoration in these three cases are $T_c = 176\mathrm{MeV}$.

It is found that all the thermodynamic properties and bulk viscosity show similar behaviors as those in the $Z(2)$ model with second order phase transition at strong coupling.

At high temperature region $T > T_c$, the behavior of the the pressure density over energy density p_T/ϵ_T, the specific heat C_v, and the trace anomaly show similar behavior as those in the symmetric case. p_T/ϵ_T increases with temperature and saturate at a value smaller than 1/3, the stronger the coupling strength is, the smaller saturation

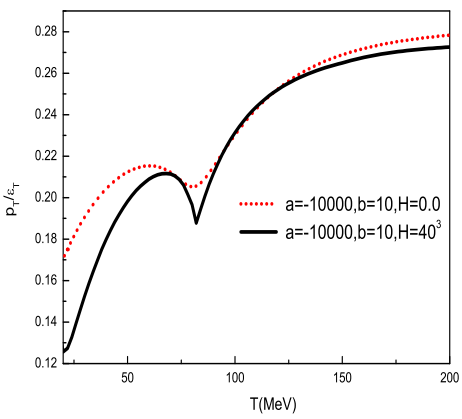

(a)

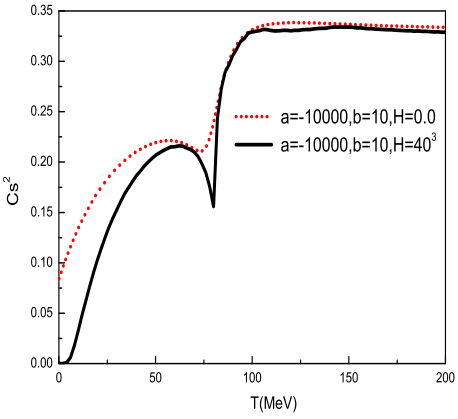

(b)

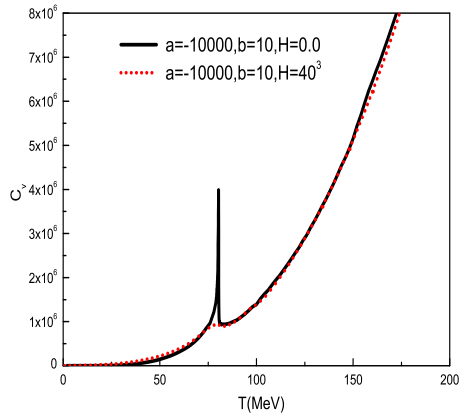

(c)

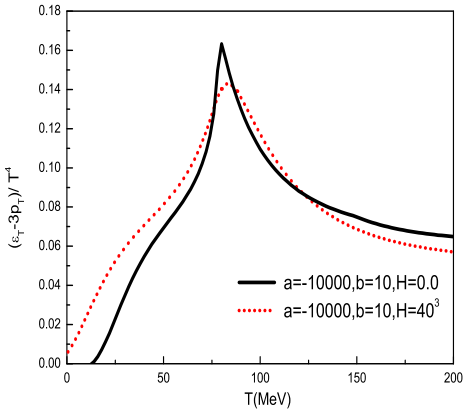

(d)

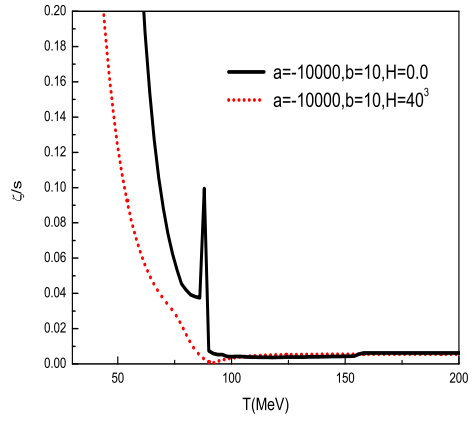

(e)

FIG. 3: The ratio of pressure density over energy density p_T/ϵ_T, the trace anomaly $(\epsilon_T - 3p_T)/T^4$, the sound velocity square C_s^2, the specific heat C_v and the bulk viscosity over entropy density ratio ζ/s as functions of the temperature T with a crossover and with a second-order phase transition in the real scalar model.

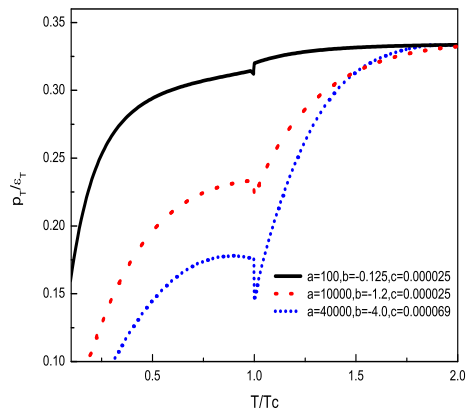

(a)

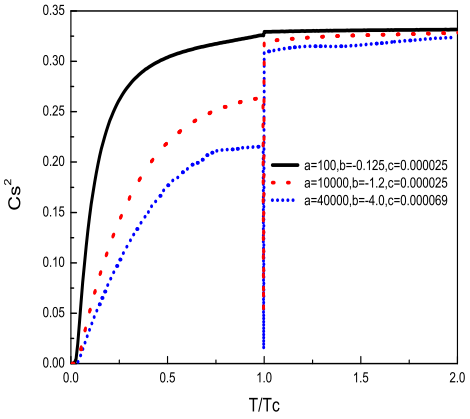

(b)

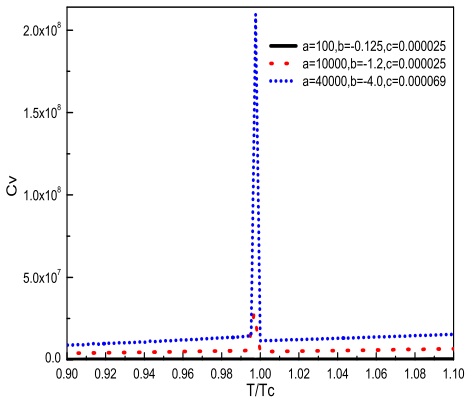

(c)

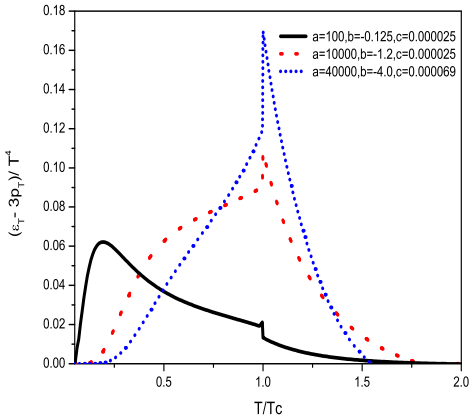

(d)

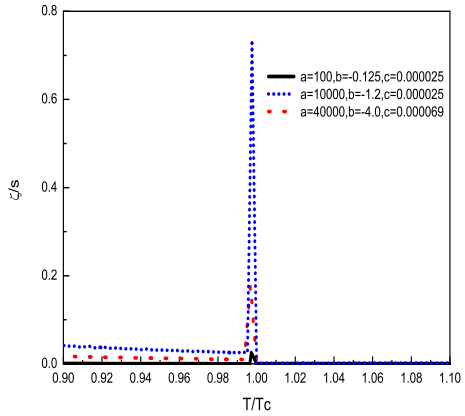

(e)

FIG. 4: The ratio of pressure density over energy density p_T/ϵ_T, the trace anomaly $(\epsilon_T - 3p_T)/T^4$, the sound velocity square C_s^2, the specific heat C_v and the bulk viscosity over entropy density ratio ζ/s as functions of the temperature T with a first-order phase transition in the real scalar model.

value p_T/ϵ_T will be. The specific heat C_v increases with temperature. The trace anomaly decreases with temperature and goes to a larger value for stronger coupling strength b. However, it is found that the sound velocity square C_s^2 shows different behavior comparing with that in the $Z(2)$ case, C_s^2 decreases with the temperature in the region $T > T_c$ in the $O(4)$ model and saturates at a value smaller than 1/3.

At low temperature region $T < T_c$, both the pressure density over energy density p_T/ϵ_T and the sound velocity square C_s^2 show a bump. There is no low-T peak showing up in the trace anomaly, because all these three sets of parameters correspond to strong coupling.

Near phase transition region $T \simeq T_c$, both the pressure density over energy density p_T/ϵ_T and the sound velocity square C_s^2 show a downward-cusp at T_c, the specific heat C_v and the trace anomaly show an upward-cusp at T_c. When the coupling strength increases, the corresponding values of the pressure density over energy density p_T/ϵ_T and the sound velocity square C_s^2 at T_c become smaller and smaller, while the critical values of the specific heat C_v and the trace anomaly become larger and larger.

The bulk viscosity over entropy density ζ/s decreases with T at low temperature region, then rises up at the critical temperature T_c. The critical value of ζ/s at T_c in the $O(4)$ model which simulates the real QCD chiral phase transition is around $0.02 - 0.06$, which is rather small comparing with the lattice QCD results.

F. $O(4)$ model with explicit symmetry breaking

In Fig. 6 $a - e$, we show the ratio of pressure density over energy density p_T/ϵ_T, the square of sound velocity C_s^2, the trace anomaly $(\epsilon_T - 3p_T)/T^4$, the specific heat C_v and the bulk viscosity over entropy density ζ/s as functions of the temperature T for the $O(4)$ model in the case of crossover when chiral symmetry is explicitly broken by a finite value $H = (121.6\text{MeV})^3$. The parameters used for calculation are taken from [37]: 1) $a = -(225.41\,\text{MeV})^2$, $b = 32.12$, 2) $a = -(388.34\,\text{MeV})^2$, $b = 76.17$, and 3) $a = -(539.27\text{MeV})^2$, $b = 145.02$, which produce the vacuum pion mass $m_\pi = 139.5\,\text{MeV}$, the vacuum pion decay constant $f_\pi = 92.4\,\text{MeV}$, and vacuum sigma meson mass as $m_\sigma = 400\text{MeV}$ $m_\sigma = 600\text{MeV}$ and $m_\sigma = 800\text{MeV}$, respectively.

At both low temperature region $T < T_c$ and high temperature region $T > T_c$, the behavior of all the thermodynamic quantities and bulk viscosity over entropy density ratio show similar behavior as the case of second order phase transition in the $O(4)$ model. However, near critical temperature region $T \simeq T_c$, it is observed all the cusp behaviors are washed out, e.g. the downward cusp in the pressure density over energy density p_T/ϵ_T and the sound velocity square C_s^2 develops into a shallow valley, and the upward cusp in the specific heat and the trace anomaly develops into a smooth peak. The sharp rise of the bulk viscosity over entropy density ζ/s in the case $H = 0$ vanishes in the chiral symmetry explicitly breaking case and there is no obvious change of ζ/s near the critical temperature. Together with the observation in the $Z(2)$ model, we can predict that at RHIC, where there is no real phase transition and the system experiences a crossover, the bulk viscosity over entropy density is small, and it will not affect too much on hadronization.

V. DISCUSSIONS AND SUMMARY

A. Comparing with other results in AdS/CFT, lattice QCD and effective QCD models

We have investigated the thermodynamic properties and bulk viscosity in the $Z(2)$ and $O(4)$ models in the Hartree approximation of CJT formalism. We now compare our results with the results in AdS/CFT, lattice QCD and effective QCD models like the Polyakov-loop Nambu–Jona-Lasinio (PNJL) model.

The conformal limit has attracted much attention in recent years, since people are trying to understand strongly interacting quark-gluon plasma by using AdS/CFT techniques. In conformal field theories including free field theory, the pressure density over energy density and the sound velocity square is always 1/3, i.e. $p_T/\epsilon_T = c_s^2 = 1/3$, and the trace anomaly and the bulk viscosity is always zero, i.e. $\Delta = \zeta = 0$. Lattice results show that at asymptotically high temperature, the hot quark-gluon system is close to a conformal and free ideal gas. Our results of $Z(2)$ and $O(4)$ models in the weak coupling also reach the conformal limit at high temperature.

However, lattice results show that near deconfinement phase transition, the hot quark-gluon system deviates far away from conformality. Both p_T/ϵ_T and c_s^2 show a minimum around 0.07, which is much smaller than 1/3. For the $SU(3)$ pure gluon system[22], the peak value of the trace anomaly Δ_{LAT}^G reads $3 \sim 4$ at T_{max} and the corresponding "interaction measure" is $\Delta_{LAT}^G/d_G = 0.2 \sim 0.25$, with the gluon degeneracy factor $d_G = 16$. (Note that here $T_{max} \simeq 1.1T_c$ is the temperature corresponding to the sharp peak of Δ.) For the two-flavor case [23], the lattice result of the peak value of the trace anomaly $\Delta_{LAT}^{Nf=2}$ reads $8 \sim 11$, the corresponding interaction measure at T_{max} is given

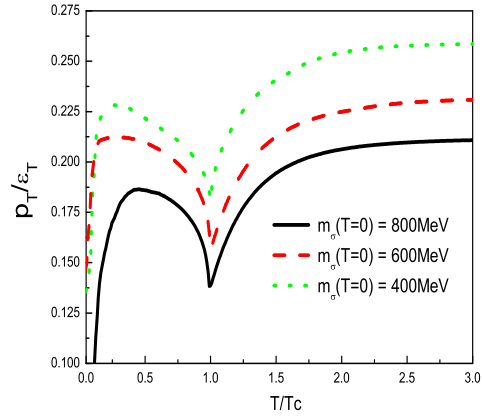

(a)

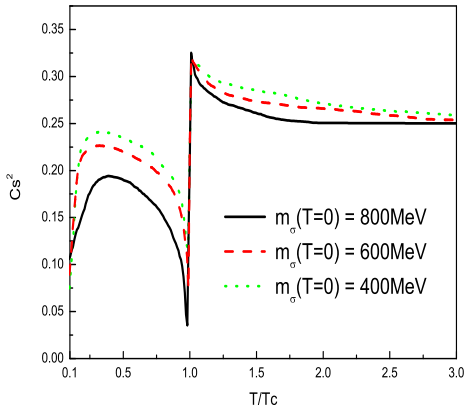

(b)

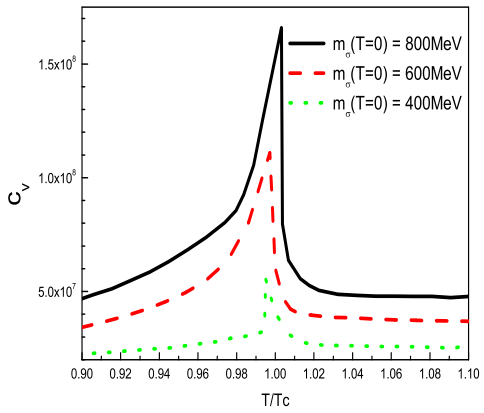

(c)

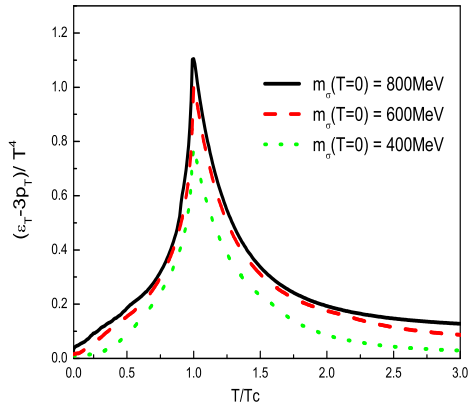

(d)

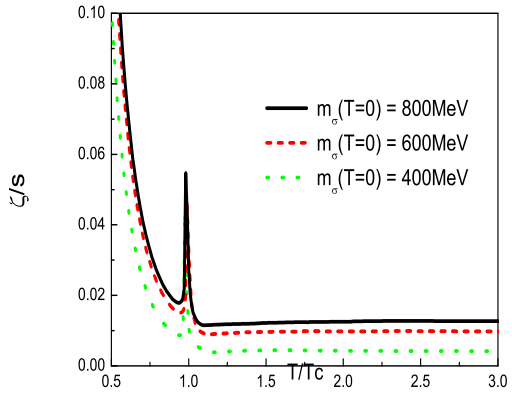

(e)

FIG. 5: The ratio of pressure density over energy density p_T/ϵ_T, the trace anomaly $(\epsilon_T - 3p_T)/T^4$, the sound velocity square C_s^2, the specific heat C_v and the bulk viscosity over entropy density ratio ζ/s as functions of the temperature T with second order phase transition in the $O(4)$ model.

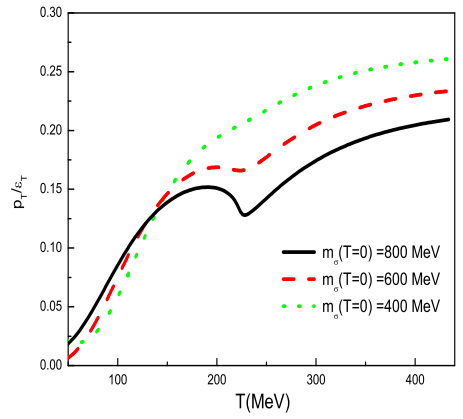

(a)

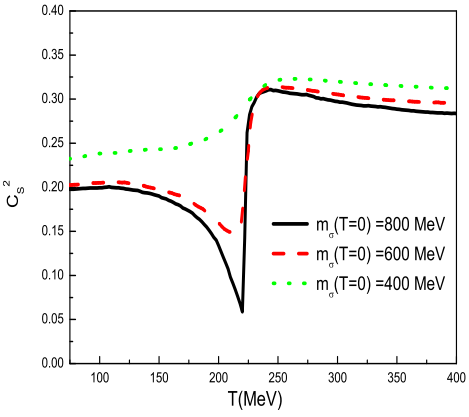

(b)

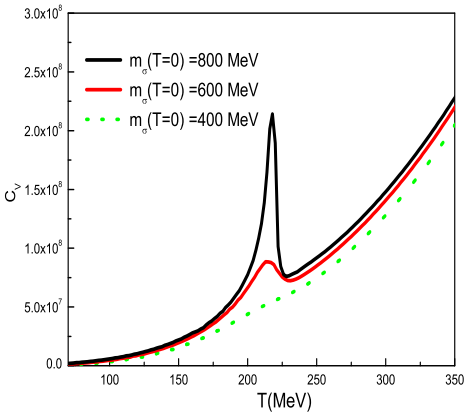

(c)

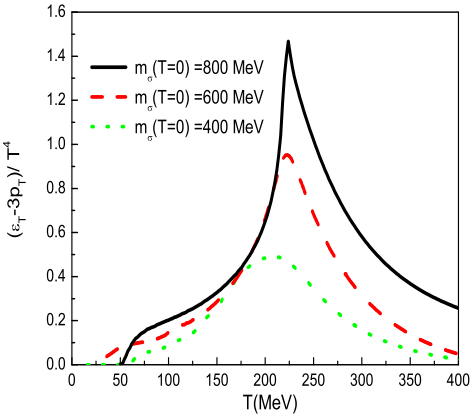

(d)

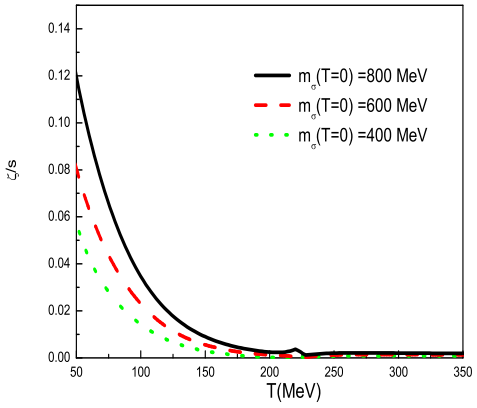

(e)

FIG. 6: The ratio of pressure density over energy density p_T/ϵ_T, the trace anomaly $(\epsilon_T - 3p_T)/T^4$, the sound velocity square C_s^2, the specific heat C_v and the bulk viscosity over entropy density ratio ζ/s as functions of the temperature T with explicit symmetry breaking in the $O(4)$ model.

as $\Delta_{LAT}^{Nf=2}/(d_G+d_Q)=0.28\sim 0.4$, with quark degeneracy factor $d_Q=12$. There have been some efforts trying to understand trace anomaly in gluodynamics near and above T_c in terms of dimension two gluon condensate and an effective "fuzzy" bag model [38].

Our results in $Z(2)$ and $O(4)$ models show that at critical temperature T_c, the trace anomaly Δ, the specific heat C_v as well as bulk viscosity to entropy density ratio ζ/s show upward cusp at T_c, and their peak values increase with the increase of coupling strength. The ratio of pressure density over energy density p_T/ϵ_T and the square of the sound velocity C_s^2 show downward cusp at T_c, which are similar to the behavior of η/s found in Ref. [31], and the cusp values decrease with the increase of coupling strength. These cusp behaviors at phase transition resemble lattice QCD results.

To our surprise, we find that when $b=30$, the strongly coulped real scalar system can reproduce all thermodynamic and transport properties of hot quark-gluon system near T_c. p_T/ϵ_T at T_c is close to the lattice QCD result 0.07, $\Delta/d=0.48$ ($d=1$ for scalar system) at T_c is close to the lattice result of the peak value $\Delta_{LAT}^{Nf=2}/(d_G+d_Q)\simeq 0.4$ at T_{max}. The bulk viscosity to entropy density ratio ζ/s at T_c is around $0.5\sim 2.0$, which agrees well with the lattice result in Ref. [16]. (Note, here $\zeta/s=0.5,2$ correspond to $\omega_0=10T,2.5T$, respectively.) More surprisingly, the shear viscosity over entropy density ratio η/s at T_c is 0.146, which also beautifully agrees with lattice result $0.1\sim 0.2$ in Ref. [11].

Table I shows our results of equation of state and transport properties in the real scalar field theory or $Z(2)$ model at T_c for second order phase transition, and corresponding results in lattice QCD calculations [15, 16, 22, 23], the PNJL model [39, 40], and black hole duals [29]. In black hole solutions, it is found that $\zeta/\eta\simeq 2(1/3-C_s^2)$. In the real scalar model near phase transition, there is no any universal relationship between ζ and η.

	η/s	ζ/s	Δ/d	C_s^2	p_T/ϵ_T
$b=30$	0.146	$0.5\sim 2.0$	0.48	0.03	0.07
LAT_G [15, 22]	$0.1\sim 0.2$	$0.5\sim 2.0$	0.25	–	0.07
$\mathrm{LAT}_{Nf=2}$ [15, 23]	–	$0.25\sim 1.0$	0.4	0.05	0.07
PNJL [39, 40]	–	–	0.21	0.08	0.075
AdS/CFT [9]	$1/4\pi$	0	0	1/3	1/3
TypeIBH [29]	$1/4\pi$	0.06	–	0.05	–
TypeIIBH [29]	$1/4\pi$	0.08	–	$\simeq 0$	–

TABLE I: Thermodynamic and transport properties at $T/T_c=1$ in $Z(2)$ at strong coupling $b=30$, in lattice QCD [15, 16, 22, 23], PNJL model [39, 40], and black hole dules [29]. The degeneracy factor $d=1,16,28$ for $Z(2)$ model, pure gluon system, and 2-flavor quark-gluon system, respectively. Lattice results are taken at T_{max}.

B. Low-T peak of the trace anomaly

In the $Z(2)$ model, it is found that the trace anomay $(\epsilon_T-3p_T)/T^4$ shows a peak at low temperature in the case of weak coupling, and this low-T peak disappears in the strong coupling case.

The peak of the trace anomaly $(\epsilon_T-3p_T)/T^4$ at low temperature, which is not related to the phase transition, was also observed in Ref. [24] in the Chiral Perturbation Theory for the pion gas. In Ref. [24], the low-T peak of the trace anomaly was interpreted as the explicit conformal breaking, whose contribution comes from massive pions. However, for the real scalar system, there are no massive pions, it is not clear for us what is the reason inducing the conformal symmetry breaking at low temperature.

We don't observe the correlation between the low-T peak of the trace anomaly and the bulk viscosity. It might be due to the method we have used to calculate the bulk viscosity. It is worthy of checking whether the correlation really exists by using Kubo formula to calculate the bulk viscosity.

C. ζ/s at RHIC

Recent lattice QCD results show that the bulk viscosity over entropy density ratio ζ/s rises dramatically up to the order of 1.0 near the critical temperature T_c [15, 16]. The sharp rise of the bulk viscosity will lead to the breakdown of the hydrodynamic approximation around the critical temperature, and will affect the hadronization and freeze-out processes of QGP created at heavy ion collisions. The authors of Ref. [25] pointed out the possibility that a sharp rise of bulk viscosity near phase transition induces an instability in the hydrodynamic flow of the plasma, and this

mode will blow up and tear the system into droplets. Another scenario is pointed out in Ref. [15, 27] that the large bulk viscosity near phase transition might induce "soft statistical hadronization".

However, if the strongly coupled QGP created at RHIC experiences a crossover and not a real phase transition, from our results in the simple $Z(2)$ and $O(4)$ models, the sharp rise of the bulk viscosity over entropy density will be washed out. In this case, one does not need to worry about the breakdown of the hydrodynamic approximation around the critical temperature.

D. Using ζ/s to locate the CEP

For real QCD with two quarks of small mass, it is expected that there exists a critical end point (CEP) in the $T-\mu$ QCD phase diagram. At small baryon chemical potential μ, the chiral phase transition is a smooth crossover at finite temperature. At finite baryon chemical potential, the chiral phase transition is of first order. The precise location of the CEP is still unknown. In the future plan, RHIC is going to lower the energy and trying to locate the CEP. Recently, the authors of Ref. [6] suggested using the shear viscosity over entropy density ratio η/s to locate the CEP.

From Refs.[31, 32], we know that η/s shows a shallow valley in the case of crossover and a jump at T_c for first-order phase transition. But it is hard to distinguish whether the system experiences a crossover or first-order phase transition just from the value of η/s extracted from the elliptic flow v_2.

From our results in $Z(2)$ and $O(4)$ models, it is found that the ratio of ζ/s shows a very sharp peak at T_c, and there is no obvious change of ζ/s for crossover. As pointed out in Ref. [25] that a sharp rise of bulk viscosity near phase transition induces an instability in the hydrodynamic flow of the plasma, and this mode will blow up and tear the system into droplets. Therefore, one can distinguish whether the system experiences a first order phase transition or a crossover from observables at RHIC experiments.

Therefore, ζ/s is a better quantity than η/s to locate the CEP. (It is noticed that because the QGP created at RHIC is a finite system, we don't discuss the singularity of $\eta/s, \zeta/s$ at CEP.)

E. Limitations of our results

At the end, we hope to point out some limitations of our results.

Firstly, the results of thermodynamic properties in this paper are based on Hartree approximation in the CJT formalism. As we know that mean-field approximation cannot describe critical phenomena very well. For 2nd-order phase transition in $Z(2)$ model, the specific heat C_v should diverge at the critical point, and behave as $t^{-\alpha}$ near the critical point, with $t=(T-T_c)/T_c$ and $\alpha=0.11$. However, in Hartree approximation of CJT formalism, though we observe the weak divergence of C_v at T_c in the case of strong coupling, we can only see a weak upward cusp of C_v at T_c in the case of weak coupling. As pointed out in the introduction, the QGP created at RHIC is a finite system, the singularity of $\eta/s, \zeta/s$ at critical point will not show up in the observables. If we are only interested in the qualitative properties near phase transition, the Hartree approximation can give the dominant contributions.

Secondly, the results of bulk viscosity in this paper are based on Eq. (34). The limitation of Eq. (34) has been analyzed in Refs. [41] and [17]. From Eq. (34), we see that the bulk viscosity is dominated by C_v at T_c. If C_v diverges at T_c, the bulk viscosity should also be divergent at the critical point and behave as $t^{-\alpha}$. However, the detailed analysis in the Ising model in Ref. [42] shows a very different divergent behavior $\zeta \sim t^{-z\nu+\alpha}$, with $z \simeq 3$ the dynamic critical exponent and $\nu \simeq 0.630$ the critical exponent in the Ising system.

Thirdly, we should keep in mind that our results at strong coupling are from effective theory. From renormalization analysis, the scalar theory will hit a Landau pole when $\beta_b > b$ with the β function $\beta_b = 9b^2/16\pi^2$. The results for large b in the scalar theory are not guaranteed to be valid in the CJT formalism.

More careful study on thermodynamic properties in this model beyond mean-field approximation is needed, and the bulk viscosity with full spectral function of the pressure-pressure correlator is in progress.

F. Summary

In summary, in the Hartree approximation of CJT formalism, we have investigated the thermodynamic properties and transport properties of the $Z(2)$ model and $O(4)$ model, and compared these properties in the cases of first and second order phase transitions, in the case of crossover and the case of symmetric phase.

We have seen that at phase transition, the system either in weak coupling or strong coupling shows some common properties. 1) The pressure density over energy density ratio p_T/ϵ_T, the square of the speed of sound C_s^2 as well as η/s exhibit downward cusp behavior at T_c. 2) The trace anomaly Δ, the specific heat C_v as well as ζ/s show upward

cusp behavior at T_c. The cusp behavior is related to the biggest change rate of entropy density at T_c [43]. 3) The cusp behavior in the first order phase transition is sharper and narrower than that in the second order phase transition. 4) In the case of crossover, the cusp behavior is washed out.

Therefore, if the strongly coupled QGP created at RHIC experiences a crossover and not a real phase transition, one does not need to worry about the breakdown of the hydrodynamic approximation around the critical temperature. Because the behavior of ζ/s is so different in the case of first order phase transition and the crossover, we also suggest that ζ/s is a better quantity than η/s to locate the CEP.

Acknowledgments

This work is supported by CAS program "Outstanding young scientists abroad brought-in", CAS key project KJCX3-SYW-N2, NSFC10735040, NSFC10875134 and NSFC10675077.

[1] Z. Fodor and S. D. Katz, J. High Energy Phys. **0203**, 014 (2002), P. de Forcrand and O. Philipsen, Nucl. Phys. Proc. Suppl. **129**, 521 (2004), F. Karsch, C. R. Allton, S. Ejiri, S. J. Hands, O. Kaczmarek, E. Laermann, and C. Schmidt, Nucl. Phys. Proc. Suppl. **129**, 614 (2004).
[2] M. Asakawa and K. Yazaki, Nucl. Phys. A **504**, 668 (1989), A. Barducci, R. Casalbuoni, G. Pettini and R. Gatto, Phys. Rev. D **49**, 426 (1994), J. Berges and K. Rajagopal, Nucl. Phys. B **538**, 215 (1999), M. A. Halasz, A. D. Jackson, R. E. Shrock, M. A. Stephanov and J. J. M. Verbaarschot, Phys. Rev. D **58**, 096007 (1998), P. Zhuang, M. Huang and Z. Yang, Phys. Rev. C **62**, 054901 (2000), O. Scavenius, A. Mocsy, I. N. Mishustin and D. H. Rischke, Phys. Rev. C **64**, 045202 (2001), N. G. Antoniou and A. S. Kapoyannis, Phys. Lett. B **563**, 165 (2003).
[3] R.D. Pisarski and F. Wilczek, Phys. Rev. D **29**, 338 (1984).
[4] Y. Hatta and T. Ikeda, Phys. Rev. D **67**, 014028 (2003), D. T. Son and M. A. Stephanov, Phys. Rev. D **70**, 056001 (2004), H. Fujii, Phys. Rev. D **67**, 094018 (2003), H. Fujii and M. Ohtani, Phys. Rev. D **70**, 014016 (2004), H. Fujii and M. Ohtani, hep-ph/0401028, K. Yagi, T. Hatsuda, Y. Miake, "Quark-Gluon Plasma, from big bang to little bang", Cambridge University Press.
[5] M. A. Stephanov, K. Rajagopal, and E. V. Shuryak, Phys. Rev. Lett. **81**, 4816 (1998). M. A. Stephanov, K. Rajagopal, and E. V. Shuryak, Phys. Rev. D **60**, 114028 (1999).
[6] R. A. Lacey *et al.*, Phys. Rev. Lett. **98**, 092301 (2007).
[7] I. Arsene *et al.* [BRAHMS Collaboration], Nucl. Phys. A **757**, 1 (2005), K. Adcox *et al.* [PHENIX Collaboration], Nucl. Phys. A **757**, 184 (2005), B. B. Back *et al.*, Nucl. Phys. A **757**, 28 (2005), J. Adams *et al.* [STAR Collaboration], Nucl. Phys. A **757**, 102 (2005).
[8] M. Gyulassy and L. McLerran, Nucl. Phys. A **750**, 30 (2005).
[9] G. Policastro, D. T. Son and A. O. Starinets, Phys. Rev. Lett. **87**, 081601 (2001), P. Kovtun, D. T. Son and A. O. Starinets, Phys. Rev. Lett. **94**, 111601 (2005).
[10] D. Teaney, J. Lauret and E. V. Shuryak, Phys. Rev. Lett. **86**, 4783 (2001), P. Huovinen, P. F. Kolb, U. W. Heinz, P. V. Ruuskanen and S. A. Voloshin, Phys. Lett. B **503**, 58 (2001), T. Hirano, U. W. Heinz, D. Kharzeev, R. Lacey and Y. Nara, Phys. Lett. B **636**, 299 (2006), P. Romatschke and U. Romatschke, Phys. Rev. Lett. **99**, 172301 (2007), H. Song and U. W. Heinz, Phys. Lett. B **658**, 279 (2008), H. Song and U. W. Heinz, Phys. Rev. C **77**, 064901 (2008).
[11] A. Nakamura and S. Sakai, Phys. Rev. Lett. **94**, 072305 (2005).
[12] P. Arnold, G. D. Moore and L. G. Yaffe, JHEP **0305**, 051 (2003).
[13] Z. Xu and C. Greiner, Phys. Rev. Lett. **100**, 172301 (2008).
[14] P. Arnold, C. Dogan and G. D. Moore, Phys. Rev. D **74**, 085021 (2006).
[15] D. Kharzeev and K. Tuchin, arXiv:0705.4280 [hep-ph]. F. Karsch, D. Kharzeev and K. Tuchin, Phys. Lett. B **663**, 217 (2008).
[16] H. B. Meyer, Phys. Rev. Lett. **100**, 162001 (2008).
[17] K. Huebner, F. Karsch and C. Pica, arXiv:0808.1127 [hep-lat].
[18] K. Paech and S. Pratt, Phys. Rev. C **74**, 014901 (2006).
[19] B. C. Li and M. Huang, Phys. Rev. D **78**, 117503 (2008).
[20] J. W. Chen and J. Wang, arXiv:0711.4824 [hep-ph].
[21] C. Sasaki and K. Redlich, arXiv:0811.4708 [hep-ph].
[22] G. Boyd, J. Engels, F. Karsch, E. Laermann, C. Legeland, M. Lutgemeier and B. Petersson, Nucl. Phys. B **469**, 419 (1996).
[23] M. Cheng *et al.*, Phys. Rev. D **77**, 014511 (2008).
[24] D. Fernandez-Fraile and A. G. Nicola, arXiv:0809.4663 [hep-ph].
[25] G. Torrieri, B. Tomasik and I. Mishustin, Phys. Rev. C **77**, 034903 (2008); G. Torrieri and I. Mishustin, arXiv:0805.0442 [hep-ph].
[26] R. J. Fries, B. Muller and A. Schafer, Phys. Rev. C **78**, 034913 (2008).
[27] T. Brasoveanu, D. Kharzeev and M. Martinez, arXiv:0901.1903 [hep-ph].

[28] J. I. Kapusta, arXiv:0809.3746 [nucl-th].
[29] S. S. Gubser, A. Nellore, S. S. Pufu and F. D. Rocha, Phys. Rev. Lett. **101**, 131601 (2008). S. S. Gubser, S. S. Pufu and F. D. Rocha, JHEP **0808**, 085 (2008).
[30] J.M. Cornwall, R. Jackiw, and E. Tomboulis, Phys. Rev. D **10**, 2428 (1974).
[31] J. W. Chen, M. Huang, Y. H. Li, E. Nakano and D. L. Yang, Phys. Lett. B **670**, 18 (2008).
[32] L. P. Csernai, J. I. Kapusta and L. D. McLerran, Phys. Rev. Lett. **97**, 152303 (2006).
[33] E. Braaten and R.D. Pisarski, Phys. Rev. Lett. **64**, 1338 (1990); Nucl. Phys. **B337**, 569 (1990).
[34] J. M. Luttinger and J. C. Ward, Phys. Rev. **118**, 1417 (1960).
[35] G. Baym, Phys. Rev. **127**, 1391 (1962).
[36] J. T. Lenaghan and D. H. Rischke, J. Phys. G **26** ,431 (2000); D. Röder, J. Ruppert, D. H. Rischke, Nucl. Phys. A **775**,127 (2006).
[37] D. Roder, arXiv:hep-ph/0509232.
[38] E. Megias, E. Ruiz Arriola and L. L. Salcedo, JHEP **0601**, 073 (2006), R. D. Pisarski, Prog. Theor. Phys. Suppl. **168**, 276 (2007).
[39] C. Ratti, M. A. Thaler and W. Weise, Phys. Rev. D **73**, 014019 (2006).
[40] S. K. Ghosh, T. K. Mukherjee, M. G. Mustafa and R. Ray, Phys. Rev. D **73**, 114007 (2006).
[41] G. D. Moore and O. Saremi, JHEP **0809**, 015 (2008).
[42] A. Onuki, Phys. Rev. E **55**, 403 (1997).
[43] M. Asakawa and T. Hatsuda, Phys. Rev. D **55**, 4488 (1997)